J Mol Model (2013) 19:205–213
DOI 10.1007/s00894-012-1530-0

ORIGINAL PAPER

Anion recognition by azophenol thiourea-based chromogenic sensors: a combined DFT and molecular dynamics investigation

Ming Wah Wong · Huifang Xie · Soo Tin Kwa

Received: 25 February 2012 / Accepted: 5 July 2012 / Published online: 31 July 2012

Abstract The relative binding affinities of several anions towards 2-nitroazophenol thiourea-based receptors were studied using density functional theory (DFT) in the gas phase and in chloroform solvent via PCM calculations. Both receptors have five distinctive NH and OH hydrogen donor atoms. All receptor–anion complexes are characterized by five intermolecular hydrogen bonds. The binding free energies are strongly influenced by a dielectric medium, and the solvation effect alters the trend of anion binding to the receptor. The calculated order of anion binding affinity for the receptor in chloroform, $H_2PO_4^- > AcO^- > F^- > Cl^- > HSO_4^- > NO_3^-$, is in excellent accord with experimental findings. The overall order of binding affinity is attributed to the basicity of the anion, the effect of solvation, and the number of proton acceptors available. Calculations of the NMR and UV-vis spectra strongly support the experimental characterization of the receptor–anion complexes. Explicit solvent molecular dynamics simulations of selected receptor–anion complexes were also carried out. Analysis of the structural descriptors revealed that the anions were strongly bound within the binding pocket via hydrogen-bonding interactions to the five receptor protons throughout the simulation.

Keywords Anion receptor · Molecular recognition · Chromogenic sensor · DFT · Molecular dynamics

Electronic supplementary material The online version of this article (doi:10.1007/s00894-012-1530-0) contains supplementary material, which is available to authorized users.

M. W. Wong (✉) · H. Xie · S. T. Kwa
Department of Chemistry, National University of Singapore,
3 Science Drive 3,
Singapore 117543, Singapore
e-mail: chmwmw@nus.edu.sg

Introduction

Anions play fundamental roles in many biological and chemical processes and in structures such as amino acids, neutrotransmitters, enzyme substrates, co-factors, nucleic acids, etc. They are also essential ingredients used by a variety of industries related to agricultural fertilizers, food additives, and water. In recent years, environmental concerns have necessitated the development of highly selective anion sensors. As a result, there has been a considerable surge of interest in developing neutral organic receptor molecules which are capable of binding a specific anionic guest selectively [1]. One of the most popular approaches to molecular sensing involves the development of chromogenic sensors [1–3]. This type of sensor system consists of two components: a subunit that is capable of interacting with an anion, and a sensing subunit in which spectroscopic features change upon anion binding [2, 3]. These two components are either covalently attached or intermolecularly connected. When appropriately designed, chromogenic anion sensors allow the "naked eye" detection of anions without the need for any spectroscopic measurements [4–7].

Thiourea is a notably good hydrogen-bond donor and an excellent anion receptor for carboxylate and dihydrogen phosphate anions [8, 9]. Hong and co-workers have reported the anion sensing of an azophenol-thiourea-based receptor, compound **1** (R = *n*-butyl, Scheme 1) [10]. They determined the association constants for anion binding using ^{1}H NMR and UV-vis titrations in $CDCl_3$. $H_2PO_4^-$, AcO^-, and F^- were found to yield stronger complexes with receptor **1** than other anions. The anion recognition, which occurred via hydrogen-bonding interactions, was monitored by anion-complexation-induced changes in ^{1}H NMR and UV-vis absorption spectra. Although anion sensor **1** allows the colorimetric detection of $H_2PO_4^-$, AcO^-, and F^-, this sensor system does not discriminate between these anions. A dual-chromophore anion sensor

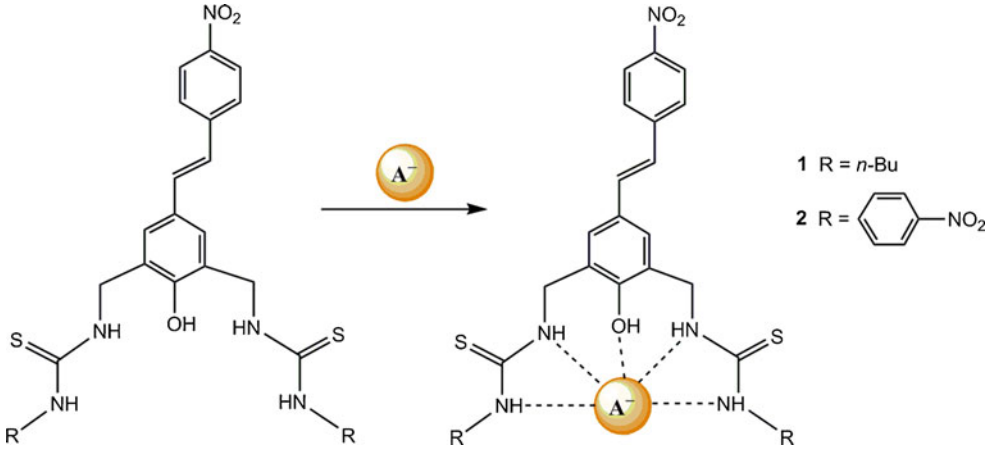

Scheme 1 Anion complexation of azophenol thiourea-based receptor (**1** or **2**)

with *p*-nitrophenylazophenol and *p*-nitrophenyl-thiourea moieties, **2** (R = $C_6H_5NO_2$, Scheme 1), was subsequently developed by Hong et al. [11]. Changing the substituents at the thiourea moieties of **1** from butyl groups to *p*-nitrophenyl groups leads to more efficient colorimetric differentiation of F^-, $H_2PO_4^-$, and AcO^-, which have similar basicities. In recent years, several azophenol-based receptors have been reported to be efficient chromogenic sensors [12, 13].

To the best of our knowledge, there are very few computational studies on chromogenic anion sensors, despite the publication of a few theoretical studies on anion recognition [4, 6, 14–18]. Theory could provide valuable insights into the structures of receptor–anion complexes, the observed binding discrimination, optical properties, and effects of solvation. It is intriguing to ask whether theory can reproduce the trend in anion binding affinity and the spectroscopic features of anion binding. Hence, we chose to investigate the anion binding of 2-nitro-azophenol thiourea-based receptors in this benchmark theoretical study. To this end, we performed density functional theory (DFT) calculations on the receptor–anion complexes between the receptors (**1** and **2**, Scheme 1) and several anions, namely fluoride, chloride, acetate, nitrate, dihydrogen phosphate, and hydrogen sulfate anions. Experimentally, the receptor–anion complexes were characterized by NMR and UV-vis spectra. Thus, we also computed the transition energies and the chemical shielding of selected receptor–anion complexes for comparison with experiment. To further shed light on the stability and conformational dynamics of the anion–receptor complexes in solvent, molecular dynamics (MD) stimulations in the presence of explicit chloroform solvent were also carried out.

Computational methods

The intermolecular complexes of azophenol-thiourea receptors (**1** and **2**) with anions (A^- = F^-, Cl^-, AcO^-, NO_3^-, $H_2PO_4^-$, and HSO_4^-) were examined by density functional theory (DFT) calculations. Geometry optimizations were performed with the hybrid B3LYP [19, 20] functional in conjunction with a split-valence polarized 6-31 G(d) basis set. Higher-level relative energies were computed at the B3LYP/6-311+G(d,p) level based on the B3LYP/6-31 G(d) optimized geometries, and included zero-point energy (ZPE) correction (B3LYP/6-31 G(d) value, scaled by a factor of 0.9804) [21]. The interaction (or binding) energy (ΔE_{int}) of the receptor–anion complex was calculated as the difference between the energy of the complex ($E_{[R\cdots A^-]}$) and the total energy of the receptor (E_R) and the anion (E_{A^-}). The binding free energy (ΔG) was computed from the equation $\Delta G_T = \Delta H_T - T\Delta S$, where ΔS is the entropy change and $\Delta H_T = \Delta H_0 + (H_T - H_0)$. The effect of solvent on the anion complexation was investigated by an implicit solvent model based on the polarizable continuum model (PCM) [22, 23]. The UAKS model was used for the molecular cavity in the PCM calculations. Both electrostatic and nonelectrostatic contributions were included in the calculated solvation free energies.

For all investigated species, a charge density analysis was performed using the natural bond orbital (NBO) approach based on the B3LYP/6-31 G(d) wavefunction [24]. NBO atomic charges of small molecules have been demonstrated to agree well with measured electron densities [25]. NMR shielding tensor spectra of **1** and its anion complexes were computed with the gauge-independent atomic orbital (GIAO) method [26, 27]. The proton chemical shifts, with tetramethylsilane (TMS) used as the reference, were computed at the B3LYP/6-311+G(d,p) level in chloroform solvent (ε=4.7). The transition energies of receptors **1** and **2** and their anion complexes were calculated using the time-dependent DFT (TD-DFT) method [28, 29] at the B3LYP/6-31+G(d) level. A recent TD-DFT study of typical chromophores using several common DFT functionals, including B3LYP, has shown that it is important to include diffuse functions when attempting to predict vertical transition energies, and the 6-31+G(d) basis set provide a good, economical choice for large systems [30]. All DFT calculations

were performed using the GAUSSIAN 03 software package [31].

Molecular dynamics simulations were carried out using the AMBER 10 program [32] for selected receptor–anion complexes in explicit chloroform solvent at room temperature. These MD calculations were accomplished using the full-atom AMBER99 (GAFF) force field [33]. The chloroform solvent molecules were described using a full-atom model [34]. Partial RESP fitted charges were derived from B3LYP/6-31 G(d) calculations. The starting geometry of the explicit solvent simulations was obtained from simulated annealing in the gas phase. The simulated annealing was performed with a starting temperature of 700 K followed by slow cooling to 0 K. This procedure was repeated several times, with the total heating time varying from 100 to 1000 ps. The resulting anion–receptor complex structure was then placed in an octahedral box of chloroform solvent molecules. The total system of solute and solvent was minimized, followed by 50 ps of NVT heating to 300 K and 50 ps of NPT equilibration at 300 K. A 1 ns production run was carried out after equilibration. The density of the equilibrated box was in close agreement with the experimental density of chloroform. The SHAKE algorithm was employed in the solvated simulations, thus allowing the use of a 2 fs time step. Nonbonded interactions were restrained to a 12 Å cutoff, and the particle mesh Ewald method was used to treat long-range electrostatic interactions. The temperature was controlled by a Langevin thermostat with a collision frequency of 1.0 ps^{-1}. The structures of the anion–receptor complexes and density distributions for both complexes and solvents were analyzed.

Discussion

Structures of anion receptors

First, we investigated the structures and energies of the azophenol-thiourea receptors **1** and **2**. To explore various possible conformations of the receptors, conformational analysis was carried out initially for **1**. The conformational search, performed at the HF/3–21 G level, was carried out using a Monte Carlo algorithm in the SPARTAN program [35]. In both receptor systems, there are two key conformations, **a** and **b**, that arise from different orientations of the two thiourea units towards the azophenol ring. The lowest-energy conformation (**1a** or **2a**) corresponds to a *trans* arrangement of the two thiourea groups (Fig. 1). This conformation (**a**) is characterized by a favorable S···H hydrogen bond between one of the thiourea sulfur atoms and the phenolic OH proton. The S···H distances in **1a** and **2a** are 2.184 and 2.210 Å, respectively. For comparison, the sum of their van der Waals radii is 2.80 Å [36]. Both sets of thiourea

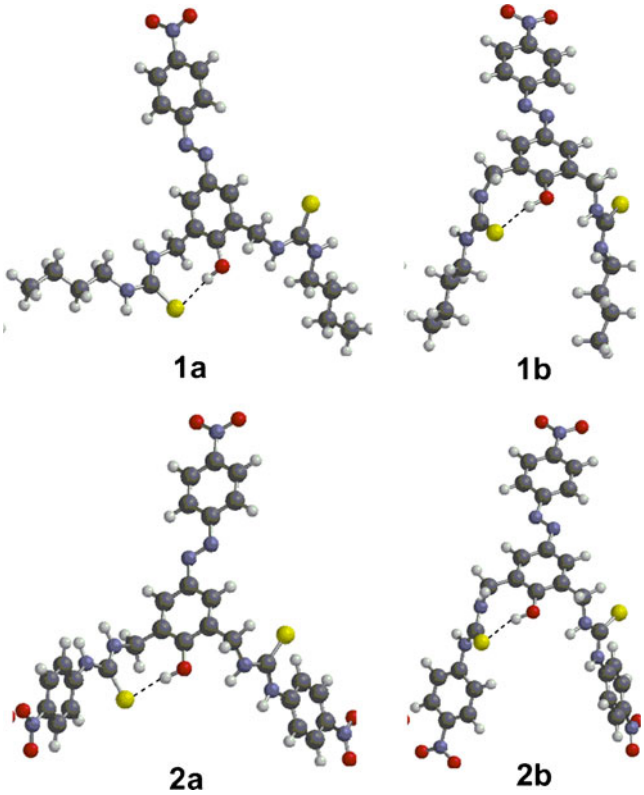

Fig. 1a–b Optimized (B3LYP/6-31 G(d)) geometries of two conformations (**a** and **b**) of azophenol-thiourea receptors (**1** and **2**). Intermolecular S···H hydrogen bonds are indicated by *dotted lines*

NH protons are in an *anti* arrangement in **1a** and **2a**. Conformer **b** is less stable than **a** by 8 and 17 kJ mol^{-1} (B3LYP/6-311+G(d,p)//B3LYP/6-31 G(d)+ZPE level) for **1** and **2**, respectively. However, conformer **b** is more important in terms of the receptor–anion interaction, since five hydrogen donor protons—namely four thiourea NH protons and one phenolic OH proton—are available within a potential binding pocket for a small anion (Fig. 1). In other words, this receptor conformation readily provides a suitable anion binding pocket with the maximum number of hydrogen-bonding donor atoms. The relative energy between the two conformations is found to be sensitive to the effect of solvation. In a dielectric medium, the relative energy of conformer **b** is significantly reduced. The calculated relative energies of **1b** and **2b** in chloroform (ε=4.9) are 5 and 4 kJ mol^{-1}, respectively. Thus, the "claw"-like conformer **b**, with two flexible thiourea arms, is easily accessible in a dielectric medium. Again, the intramolecular S···H hydrogen bond is present in both conformers, **1b** and **2b** (Fig. 1).

The two thiourea groups of the receptors are fairly flexible. To accommodate the intramolecular hydrogen bonds, both thiourea moieties are significantly distorted from planarity in conformations **a** and **b**. For instance, the calculated torsional angles of the two thiourea units (with respect to the plane of the azophenol ring) in **1a** are 64 and 87°. It is

important to note that the thiourea NH protons and phenolic OH proton bear strong positive charges, 0.42–0.51 au, in both receptors. Thus, **1b** and **2b** are characterized by five strong hydrogen-bond donor atoms. The positions of the five protons suggest that the receptor can readily bind with three oxygen atoms of the tetrahedral anions $H_2PO_4^-$ and HSO_4^-. All receptor conformations are characterized by a fairly large dipole moment of >10 debyes.

Structures and interaction energies of receptor–anion complexes

Next, we examined the structures and binding energies of the 1:1 complexes between the azophenol-thiourea receptor **2** and various anions (F^-, Cl^-, AcO^-, NO_3^-, $H_2PO_4^-$, and HSO_4^-). In receptor **2**, one phenol OH and four thiourea NH protons could function as anion-binding moieties. As shown for the optimized geometries of all receptor–anion complexes (Fig. 2), all five receptor protons interact cooperatively with various anions through hydrogen bonds. The intermolecular hydrogen-bond distances of these complexes are given in Table 1. Not surprisingly, the phenolic hydrogen bond is significantly stronger than the others, as reflected in its shorter hydrogen-bonding distance (Table 1). Interestingly, the halide ion (F^- or Cl^-) forms five X–H···A^- (X = N or O) hydrogen bonds with the receptor in a pentadentate fashion (Fig. 2). For acetate and nitrate complexes, two anion oxygens are involved in intermolecular hydrogen-bonding interactions. One oxygen interacts simultaneously with the phenol proton and two NH protons of one thiourea group, while the other oxygen interacts with two NH protons of another thiourea unit. In the $H_2PO_4^-$ and HSO_4^- complexes, three out of the four anion oxygens are involved in intermolecular hydrogen bonds (Fig. 2). As expected, hydrogen bonds with the P=O or S=O oxygens are favored over the hydroxyl oxygens in the most stable forms of these complexes. Overall, both thiourea arms of receptor **2** are sufficiently flexible to accommodate anions of different sizes and to achieve maximum intermolecular interactions via hydrogen bonds. This is clearly demonstrated in the space-filling models of the anion–receptor complexes (see Fig. S1 of the "Electronic supplementary material," ESM). We note that weaker C–H···O interactions [37, 38] are also observed in the optimized geometries of the AcO^-, $H_2PO_4^-$, and HSO_4^- complexes. It is important to note that the B3LYP/6-31 G(d) optimized geometries of various anion–receptor complexes are sufficiently reliable, based on comparisons with larger basis-set optimizations, namely those utilizing 6-31+G(d), 6-31 G(d,p), 6-31+G(d,p), 6-311+G(d,p), for the chloride complex.

The computed gas-phase ($\varepsilon = 1$) binding energies (ΔE_0, ΔH_{298}, and ΔG_{298}) of the receptor–anion complexes at the B3LYP/6-311+G(d,p)//B3LYP/6-31 G(d) level are given in Table 2. The predicted binding free energies are fairly large (>200 kJ mol^{-1}) in all cases. This high gas-phase interaction energy is not unexpected, because the hydrogen-bonding interactions involve an anionic species. For instance, the F–H···F^- complex has been found experimentally to have a substantial binding enthalpy (ΔH_{298}) of 191.6 kJ mol^{-1} [39]. This value of the F–H···F^- hydrogen-bonding interaction energy is well reproduced by the enthalpy (ΔH_{298}= 197.0 kJ mol^{-1}) calculated at the B3LYP/6-311+G(d,p)// B3LYP/6-31 G(d) level of theory [4]. This lends strong confidence to our predicted interaction energies of the various receptor–anion complexes examined in this study. The predicted order of anion binding affinity of azophenol-thiourea receptor **2** in vacuo is $F^- > AcO^- > H_2PO_4^- > Cl^- > HSO_4^- > NO_3^-$. This calculated order does not follow the normal trend in basicity for these anions [40]. A similar theoretical finding has been reported for the binding of common anions to simple thiourea [16]. F^- forms the strongest complex with receptor **2**

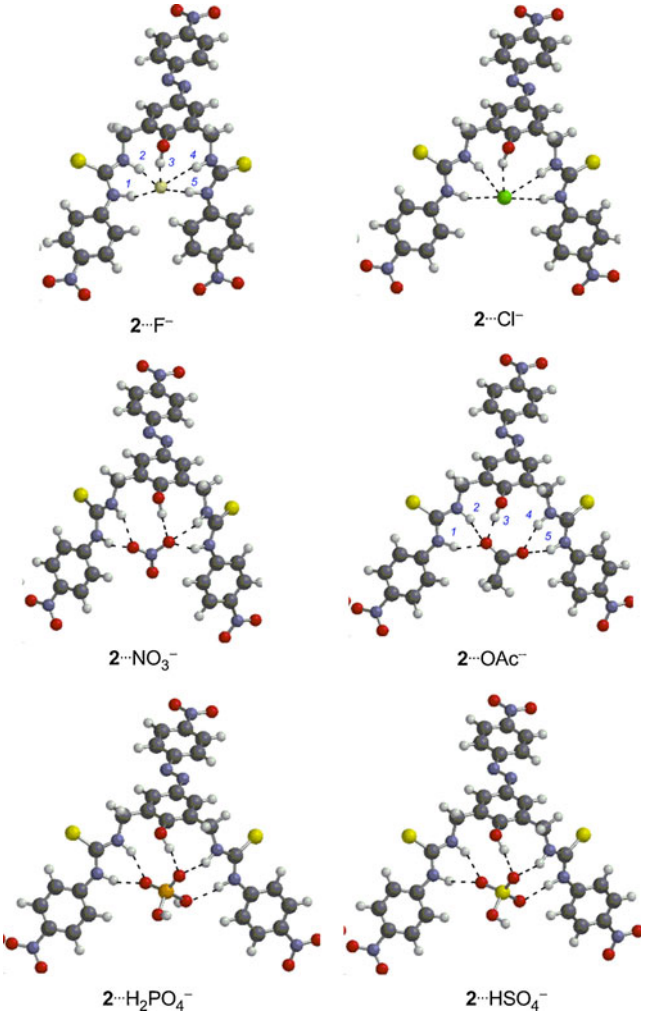

Fig. 2 Optimized (B3LYP/6-31 G(d)) geometries of various receptor–anion complexes. Intermolecular hydrogen bonds are indicated by *dotted lines*

Table 1 Calculated hydrogen-bonding structural parameters of various receptor–anion complexes[a]

Species	*r*(O–H)	*r*(A···HO)	<(AHO)	*r*(A···NH)
1···F^-	1.054	1.385	166.7	1.760, 1.848, 1.848, 2.376
1···$H_2PO_4^-$	1.003	1.654	168.1	1.848, 1.942, 2.045, 2.095
2···F^-	1.024	1.486	165.5	1.703, 1.742, 1.843, 2.453
2···AcO^-	1.011	1.664	175.2	1.871, 1.905, 1.941, 1.966
2···$H_2PO_4^-$	0.999	1.680	167.3	1.826, 1.864, 1.987, 2.040
2···Cl^-	0.993	2.160	157.0	2.325, 2.334, 2.456, 2.640
2···HSO_4^-	0.989	1.747	167.1	1.926, 1.949, 1.968, 2.050
2···NO_3^-	0.995	1.746	176.3	1.885, 1.990, 2.032, 2.033

[a] B3LYP/6-31 G(d) level (gas phase); bond lengths are in Å and bond angles are in degrees

among the anions studied. Although F^-, AcO^-, and $H_2PO_4^-$ are calculated to have greater binding energies than the other anions, the order of binding affinity is different from the observed experimental trend ($H_2PO_4^- > F^- \approx AcO^-$) [11]. More importantly, the binding free energies of Cl^- and HSO_4^- (−226 and −183 kJ mol^{-1}, respectively) are too large to account for the fact that they were not observed in experimental studies [10, 11]. How do we account for this discrepancy?

Experimentally, the anion recognition of azophenol receptor **2** was carried out in chloroform solvent [10, 11]. It is well established that small anions are strongly solvated in a dielectric medium [41]. Therefore, it was crucial to investigate the influence of solvation on the binding energies of the various receptor–anion complexes. To this end, we investigated the influence of chloroform solvent (ε=4.9) on the binding free energies of the receptor–anion complexes using the polarizable continuum model (PCM). It is instructive to first examine the effect of a dielectric medium on the structure of the receptor–anion complex. For the dihydrogen phosphate complex (**2**···$H_2PO_4^-$), the optimized geometry in chloroform is fairly close to that of the gas-phase geometry. The changes in the intermolecular hydrogen-bonding distances are in the range 0.01–0.06 Å. It thus appears that the presence of a dielectric medium has only a small influence on the geometry of the receptor–anion complex. Hence, we employed gas-phase geometries to compute the interaction energies of all receptor–anion complexes in chloroform at the PCM-B3LYP/6-311+G(d,p) level. As evidenced in Table 2, the binding free energies (ΔG_{298}) decrease considerably, by 142–264 kJ mol^{-1}, upon going from the gas phase to solution. These substantial changes are not unexpected, as the small anions are strongly solvated in a dielectric medium. For instance, the calculated solvation free energy of acetate anion in chloroform is −497 kJ mol^{-1}. The differential solvent stabilization effect upon complexation leads to a significant reduction in the binding free energy of the receptor–anion complex. The calculated trend for the binding affinity in chloroform ($H_2PO_4^- > F^- > AcO^- > Cl^- > HSO_4^- > NO_3^-$) is slightly different from that in the gas phase. In particular, $H_2PO_4^-$ has the largest binding free energy (−92 kJ mol^{-1}) in chloroform. As in the isolated state, F^-, AcO^-, and $H_2PO_4^-$ bind considerably more strongly to **2** than to other anions, in accordance with the observed selective binding by the azophenol thiourea-based receptor. Most importantly, the PCM calculations correctly reproduce the observed relative binding affinities of F^-, AcO^-, and $H_2PO_4^-$ [11]. Hence, we can conclude that the overall order of binding affinity is attributable to the basicity of the anion, the effect of solvation, and the number of proton acceptors available. It is worth noting that the strength of the azophenolic hydrogen bond, as reflected in the O–H distance, correlates well with the gas-phase binding energy. This suggests that the phenolic hydrogen bond plays a key role in the anion recognition of the azophenol receptor.

Table 2 Calculated interaction energies[a] (ΔE_0, ΔH_{298}, and ΔG_{298}, in kJ mol^{-1}) of various receptor–anion complexes in the gas phase and chloroform

Complex	Gas phase (ε=1.0)		Chloroform (ε=4.9)	
	ΔE_0	ΔH_{298}	ΔG_{298}	ΔG_{298}[b]
1···F^-	−325.8	−329.9	−287.3.3	−75.8
1···$H_2PO_4^-$	−216.4	−216.1	−160.7.7	−77.5
2···F^-	−389.6	−393.4	−350.1.1	−86.5
2···AcO^-	−292.6	−290.5	−239.5.5	−75.4
2···$H_2PO_4^-$	−279.9	−279.3	−227.4.4	−92.0
2···Cl^-	−260.1	−260.8	−225.7.7	−46.0
2···HSO_4^-	−240.1	−239.2	−183.0.0	−41.3
2···NO_3^-	−231.5	−231.2	−180.3.3	−23.0

[a] Based on the B3LYP/6-311+G(d,p)//B3LYP/6-31 G(d) level of theory

[b] Solvation calculations were performed using the PCM method

To further examine the effect of substitution in the azophenol-thiourea derivatives, we also examined the fluoride and dihydrogen phosphate complexes of receptor **1** (Scheme 1) with an *n*-butyl substituent (i.e., **1**···F^- and **1**···$H_2PO_4^-$). Their optimized geometries are similar to the corresponding anion complexes with receptor **2**. However,

the intermolecular N–H···O hydrogen-bonding distances are significantly longer in both cases (Table 1). Accordingly, the calculated binding free energies (ΔG_{298}) in chloroform are smaller than the corresponding fluoride and phosphate complexes with **2**, by 11 and 15 kJ mol^{-1}, respectively (Table 2). Hence, our calculations confirm the enhanced hydrogen-bonding ability of *p*-nitrophenyl groups in receptor **2** compared to **1**. Consistent with experimental findings [10], both F^- and $H_2PO_4^-$ have similar binding free energies to receptor **1**.

Finally, we note that all the receptor–anion complexes examined here are characterized by a large dipole moment (Table S1 of the ESM), particularly for the nitrate complex. Based on NBO charge density analysis, a significant degree of charge transfer (from the anion to the receptor) is calculated to occur in all of the complexes (Table S1). The amount of charge transfer is in the range 0.17–0.31 au. Interestingly, the magnitude of charge transfer correlates reasonably well with the gas-phase binding energy of the complex.

Molecular dynamics simulations

To further explore the stability and conformational dynamics of the receptor–anion complexes in solvent, MD simulations of selected receptor–anion complexes were run over a period of 1 ns in explicit chloroform solvent. Since a reliable AMBER force field is not available for certain anions, our dynamics study investigated only the fluoride and acetate complexes (i.e., **2**···F^- and **2**···AcO^-). The starting geometry of the explicit solvent simulation was obtained from simulated annealing in the gas phase, which yielded the lowest-energy conformation of the receptor–anion complex. The lowest-energy structure derived from the simulated annealing is similar to that obtained from DFT optimization. However, the intermolecular hydrogen-bonding distances are generally shorter, e.g., 1.561 (O···H), 1.800, 1.801, 1.847, and 1.907 Å in acetate complex (**2**···AcO^-). These differences, perhaps, are not unexpected, as both structures were obtained from different computational methods. Plots of the root square mean deviation (RSMD) for both fluoride and acetate complexes (Figs. S2 and S3 of the ESM) behave similarly over the 1 ns simulations, and the oscillations about a stable mean from ca. 100 ps onwards indicate that the simulations are stable over this period.

Our main strategy in analyzing the dynamics was to examine the O–H···A and N–H···A (A = anion) hydrogen-bond distances. The H···A distances were plotted as a function of time for both simulations in Fig. 3a and b for **2**···F^- and **2**···AcO^-, respectively. Upon inspecting these figures, it becomes immediately apparent that the phenolic proton is bonded to the anion tightly throughout the simulation period. In the MD simulation of the fluoride complex (**2**···F^-), the fluoride ion is essentially hydrogen bonded to the five receptor protons throughout the entire simulation run, as shown in the H···F distance plots in Fig. 3a. In other words, the fluoride ion stays tightly within the receptor binding pocket in chloroform solvent. A similar result is obtained for the acetate complex (**2**···AcO^-). In this case, the phenolic proton is hydrogen bonded to either one of the two anion oxygen atoms. Distinct switching between the two oxygens is seen during the simulation (see Fig. 3b). Thus, the phenolic proton is bonded to both oxygens in the time-averaged MD structure. Interestingly, each set of thiourea protons interacts distinctly with only one specific receptor oxygen (see Fig. 3b). This readily indicates that the acetate ion did not rotate or flip around during the simulation process. In summary, the MD simulations of both anion complexes clearly show that the anion is strongly bound within the binding pocket of the azophenol-thiourea receptor in the explicit solvent simulation. Furthermore, all five receptor protons are hydrogen bonded to the anion throughout the simulation run. Finally, an MD simulation was carried out with an acetate ion placed slightly outside the binding pocket of the receptor (**2**). As one might have expected, the anion moved into the binding pocket during the explicit solvent simulation.

Calculated NMR and UV-visible spectra

The binding ability of the azophenol-thiourea receptor **1** via hydrogen-bonding interactions was supported by ^{1}H NMR experiments in $CDCl_3$ [10]. In particular, large downfield shifts of thiourea protons (>2.5 ppm) were detected upon complexation with $H_2PO_4^-$ and AcO^-. Broadening of the phenol OH resonance was also observed, indicating its participation in hydrogen-bonding interactions with the anions. To examine how theory faired in this case, we computed the NMR spectra of receptor **1** and its dihydrogen phosphate complex (**1**···$H_2PO_4^-$) using the GIAO [26, 27] method in chloroform solvent. For receptor **1**, the calculated ^{1}H chemical shifts (with respect to TMS) of various NH protons of the two thiourea moieties in **1**, 6.9–9.4 ppm (Fig. 4), are in pleasing agreement with the experimental values [10]. In excellent accordance with the experimental findings, significant shifts of 1.7–3.0 ppm were calculated for all of the thiourea NH protons upon complexation with $H_2PO_4^-$ (Fig. 4). Accordingly, the phenolic OH proton in **1** undergoes a significant downfield shift of 2.9 ppm upon complexation (Fig. 4). These sizeable changes in proton chemical shifts are readily attributed to the decreased electron density at the NH and OH protons upon the formation of hydrogen bonds with $H_2PO_4^-$ in the receptor–anion complex. NBO charge density analysis of receptor **1** and its phosphate complex supports this rationalization. In summary, our calculated ^{1}H NMR chemical shifts confirm the observed binding ability of the azophenol thiourea-based sensor **1**.

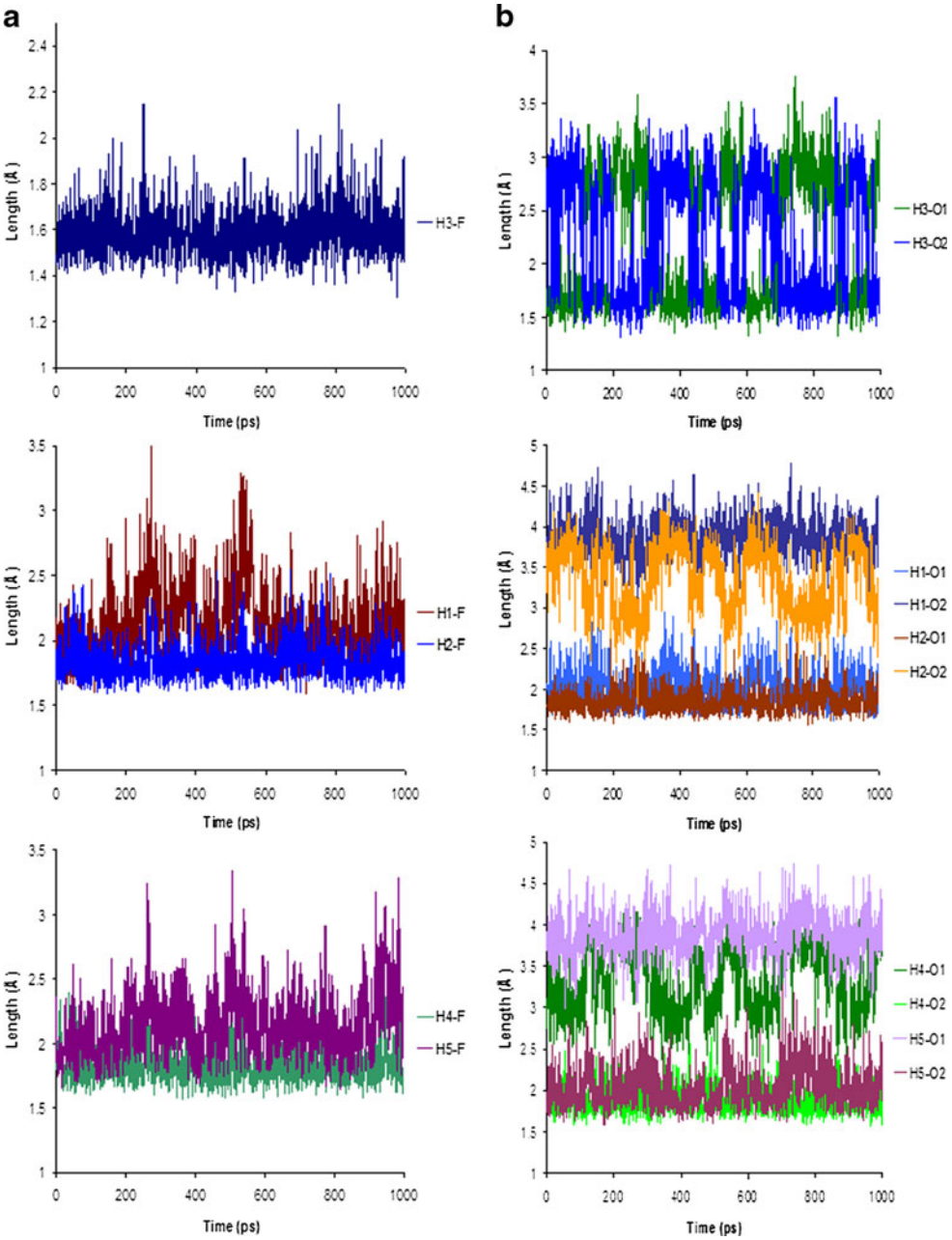

Fig. 3a–b Hydrogen-bond distances of **a** **2**···F^- and **b** **2**···AcO^- during MD simulations in chloroform. Atom labels are given in Fig. 2

In naked-eye experiments, both of the azophenol-thiourea receptors **1** and **2** underwent very dramatic color changes in the presence of $H_2PO_4^-$, AcO^-, and F^- [10, 11]. For receptor **1**, anion binding led to a notable color change from light yellow to deep red [10]. Remarkably, anion receptor **2** with dual chromophores, namely the nitrophenylazophenol and nitrophenylthiourea moieties, allows for colorimetric discrimination between $H_2PO_4^-$, AcO^-, and F^- [11]. To shed light on the nature of the UV-visible spectral changes in the presence of anions, we have calculated the absorption spectra of receptor **2** and selective anion complexes using the time-dependent DFT (TD-DFT) [28, 29] method in chloroform solvent. It is important to note that although TD-DFT reasonably successfully predicts accurate excitation spectra in a wide variety of systems [42], difficulties still plague its application to certain areas, such as the prediction of long-range charge-transfer (CT) excitations [43]. The computed transition energies of several anion complexes of receptor **2** are summarized in Table 3. The calculated spectrum of sensor **2** is characterized by two distinct sets of transitions: (1) **T1**: nitrophenylthiourea $\pi \rightarrow$ nitrophenylthiourea π^*, and (2) **T2**: thiourea sulfur lone pair $\rightarrow$ azophenol π^* (LUMO). The computed **T1** transition energies (328 and 340 nm) of **2** agree well with the observed λ_{max} value of 339 nm [11]. Surprisingly, the predicted **T2** transition is not observed in the UV-vis spectrum of **2**. Upon complexation with an anion (F^-, Cl^-, AcO^-, or

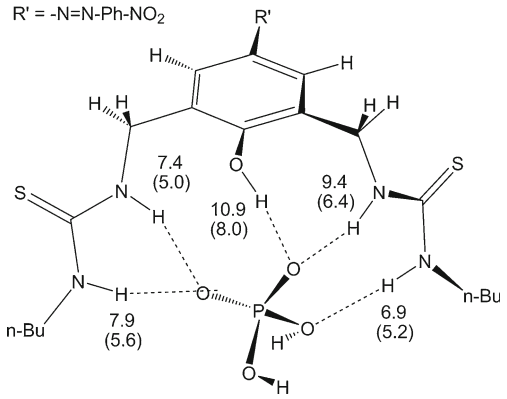

Fig. 4 Calculated (PCM-B3LYP/6-311+G(d,p)) ^{1}H chemical shifts (ppm, with respect to TMS) of **1** and **1**···$H_2PO_4^-$ in chloroform. Values for receptor **1** are given in parentheses

$H_2PO_4^-$), the characteristic absorption peaks of receptor **2** undergo a significant redshift, and a new peak appears at >500 nm (Table 3). This new absorption peak (**T3**) corresponds to the transition from azophenol π* (HOMO) to azophenol π* (LUMO). The relevant molecular orbitals involved in the **T1**, **T2**, and **T3** transitions are depicted in Fig. 5. The trend in the **T3** absorption value, $H_2PO_4^- > F^- \approx AcO^- > Cl^-$, is in pleasing accord with the experimental findings [11]. In particular, the addition of $H_2PO_4^-$ to **2** leads to the largest spectral change. We note that the calculated intensity for the **T3** (HOMO→LUMO) transition is rather low compared to the intense peak observed experimentally [11]. This is probably due to the shortcomings of the TD-DFT method. The bathochromic shift of the **T1** transition is readily due to the stabilization of the excited state by anion binding. In summary, our computational results yield good qualitative agreement with the UV absorption changes upon complexation, and confirm the experimental finding that **2** is an efficient colorimetric anion sensor.

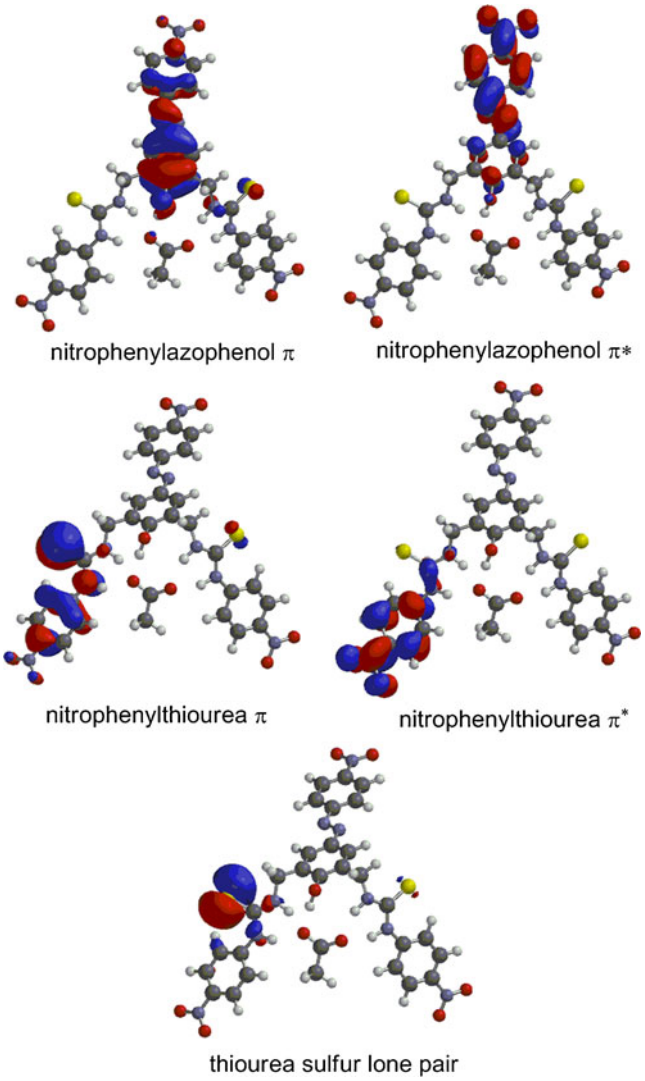

Fig. 5 Molecular orbitals related to the **T1**, **T2**, and **T3** transitions of the **2**···AcO^- complex

Concluding remarks

Density functional theory (DFT) calculations were carried out to determine the binding affinities of several common anions towards 2-nitroazophenol thiourea-based receptors **1** and **2** in the gas phase and in chloroform. Their calculated binding free energies in chloroform were substantially smaller than their corresponding gas-phase values. This

Table 3 Calculated transition energies[a,b] (nm) of receptor **2** and various receptor–anion complexes in chloroform

Species	T1	T2	T3
Assignment	Phenylthiourea π → phenylthiourea π*	Sulfur lone pair → azophenol π*	Azophenol π → azophenol π*
2	328 (0.34), 340 (0.26)	421 (0.16), 439 (0.83)	
2···Cl^-	350 (0.30), 365 (0.28)	420 (0.57), 450 (0.68)	510 (0.04)
2··· AcO^-	361 (0.34), 373 (0.37)	423 (0.29), 456 (0.75)	549 (0.06)
2··· F^-	358 (0.37), 369 (0.20)	424 (0.16), 452 (0.83)	555 (0.06)
2··· $H_2PO_4^-$	369 (0.51), 379 (0.22)	426 (0.34), 456 (0.69)	570 (0.07)

[a] Based on TD-DFT calculations performed at the PCM-B3LYP/6-31+G(d)//B3LYP/6-31 G(d) level

[b] Oscillator strength is given in parentheses

demonstrates the important role of solvation in controlling the anion-binding strength and selectivity. In the optimized geometries of the receptor–anion complexes, all five thiourea NH and phenolic OH protons of the receptors were involved in multitopic hydrogen-bonding interactions with anions. The binding between the azophenolic OH proton and the anion plays a more prominent role. In excellent agreement with experiment, $H_2PO_4^-$, AcO^-, and F^- bind significantly better than other anions. In addition, PCM calculations correctly predict the observed relative binding affinity ($H_2PO_4^- > F^- > AcO^-$). Calculated complexation-induced changes in the ^1H chemical shift are in excellent agreement with experimental results. UV-visible spectra calculations readily support the experimental characterization of the receptor–anion complexes. Explicit solvent molecular dynamics simulations reveal that the anions are strongly bound within the binding pocket via hydrogen bonds to the five receptor protons throughout the 1 ns simulation run in chloroform solvent.

Acknowledgments This research was supported by the National University of Singapore (grant no: R-143-000-253-112).

References

1. Sessler JL, Gale PA, Cho WS (2006) Anion receptor chemistry. Royal Society of Chemistry, Cambridge
2. Gunnlaugsson T, Glynn M, Tocci GM, Kruger PE, Pfeffer FM (2006) Coord Chem Rev 250:3094–3117
3. Gale PA, Quesada R (2006) Coord Chem Rev 250:3219–3244
4. Wong MW, Ghosh T, Maiya BG (2004) J Phys Chem A 108:11249–11259
5. Lee SJ, Jung JH, Seo J, Yoon I, Park KM, Lindoy LF, Lee SS (2006) Org Lett 8:1641–1643
6. Singh NJ, Jun EJ, Chellappan K, Thangadurai D, Chandran RP, Hwang IC, Yoon J, Kim KS (2007) Org Lett 9:485–488
7. Lu QS, Dong L, Zhang J, Li J, Jiang L, Huang Y, Qin S, Hu CW, Yu XQ (2009) Org Lett 11:669–672
8. Li AF, Wang JH, Wang F, Jiang YB (2010) Chem Soc Rev 39:3729–3745
9. Kato R, Nishizawa S, Hayashita T, Teramae N (2001) Tetrahedron Lett 42:5053–5056
10. Lee DH, Lee KH, Hong JI (2001) Org Lett 3:5–8
11. Lee DH, Lee HY, Lee KH, Hong JI (2001) Chem Commun 1188–1189
12. Lee DH, Im JH, Son SU, Chung YK, Hong JI (2003) J Am Chem Soc 125:7752–7753
13. Chen YJ, Chung WS (2009) Eur J Org Chem 4770–4776
14. Ruangpornvisuti VJ (2004) Mol Struct Theochem 686:47–55
15. Mondal CK, Lee JY (2006) J Theor Comput Chem 5:857–869
16. Jose DA, Singh A, Das A, Ganguly B (2007) Tetrahedron Lett 48:3695–3698
17. Rakrai W, Morakot N, Keawwangchai S, Kaewtong C, Wanno B, Ruangpornvisuti V (2011) Struct Chem 22:839–847
18. Xie H, Wong MW (2012) Aust J Chem 65:303–313
19. Becke DA (1993) J Chem Phys 98:5648–5652
20. Lee C, Yang W, Parr RG (1988) Phys Rev B 37:785–789
21. Wong MW (1996) Chem Phys Lett 256:391–399
22. Cossi M, Barone V, Cammi R, Tomasi J (1996) Chem Phys Lett 255:327–335
23. Barone V, Cossi M, Tomasi J (1997) J Chem Phys 107:3210–3221
24. Reed AE, Curtiss LA, Weinhold F (1988) Chem Rev 88:899–926
25. Messerschmidt M, Wagner A, Wong MW, Luger P (2002) J Am Chem Soc 124:732–733
26. Wolinski K, Hinton JF, Pulay P (1990) J Am Chem Soc 112:8251–8260
27. Cheeseman JR, Trucks GW, Keith T, Frisch MJ (1996) J Phys Chem 104:5497–5509
28. Bauernschmitt R, Ahlrichs R (1996) Chem Phys Lett 256:454–464
29. Casida ME, Jamorski C, Casida KC, Salahub DR (1998) J Chem Phys 108:4439–4449
30. Jacquemin D, Adamo C (2012) Int J Quantum Chem 112:2135–2141
31. Frisch MJ, Trucks GW, Schlegel HB, Scuseria GE, Robb MA, Cheeseman JR, Montgomery JA Jr, Vreven T, Kudin KN, Burant JC, Millam JM, Iyengar SS, Tomasi J, Barone V, Mennucci B, Cossi M, Scalmani G, Rega N, Petersson GA, Nakatsuji H, Hada M, Ehara M, Toyota K, Fukuda R, Hasegawa J, Ishida M, Nakajima T, Honda Y, Kitao O, Nakai H, Klene M, Li X, Knox JE, Hratchian HP, Cross JB, Bakken V, Adamo C, Jaramillo J, Gomperts R, Stratmann RE, Yazyev O, Austin AJ, Cammi R, Pomelli C, Ochterski JW, Ayala PY, Morokuma K, Voth GA, Salvador P, Dannenberg JJ, Zakrzewski VG, Dapprich S, Daniels AD, Strain MC, Farkas O, Malick DK, Rabuck AD, Raghavachari K, Foresman JB, Ortiz JV, Cui Q, Baboul AG, Clifford S, Cioslowski J, Stefanov BB, Liu G, Liashenko A, Piskorz P, Komaromi I, Martin RL, Fox DJ, Keith T, Al-Laham MA, Peng CY, Nanayakkara A, Challacombe M, Gill PMW, Johnson B, Chen W, Wong MW, Gonzalez C, Pople JA (2004) Gaussian 03. Gaussian Inc., Wallingford
32. Case DA, Darden TA, Cheatham TE III, Simmerling CL, Wang J, Duke RE, Luo R, Merz KM, Pearlman DA, Crowley M, Walker RC, Zhang W, Wang B, Hayik S, Roitberg A, Seabra G, Wong KF, Paesani F, Wu X, Brozell S, Tsui V, Gohlke H, Yang L, Tan C, Mongan J, Hornak V, Cui G, Beroza P, Mathews DH, Schafmeister C, Ross WS, Kollman PA (2006) AMBER 9. University of California, San Francisco
33. Pearlman DA, Case DA, Caldwell JW, Ross WR, Cheatham TE III, DeBolt S, Ferguson D, Seibel G, Kollman PA (1995) Comp Phys Commun 91:1–41
34. Cieplak P, Caldwell JW, Kollman PA (2001) J Comput Chem 22:1048–1057
35. Wavefunction Inc. (2010) SPARTAN 10. Wavefunction Inc., Irvine
36. Bondi A (1964) J Phys Chem 68:441
37. Desiraju GR (1991) Acc Chem Res 24:290–296
38. Ran J, Wong MW (2009) Aust J Chem 62:1062–1067
39. Wenthold PG, Squires RR (1985) J Phys Chem 99:2002–2005
40. Wiskur SL, Ait-Haddou H, Lavigne JJ, Anslyn EV (2001) Acc Chem Res 34:963–972
41. Böes ES, Andrade JA, Stassen H, Goncalves PFB (2007) Chem Phys Lett 436:362–367
42. Marques MAL, Ullrich CA, Nogueira F, Rubio A, Burke K, Gross EKU (eds) (2006) Time-dependent density functional theory. Springer, Berlin
43. Dreuw A, Weisman J, Head-Gordon M (2003) J Chem Phys 119:2943–2946